

# Assessing Contrast Sensitivity Function in *CRB1*-Retinopathies: Exploring Child-Friendly Measures of Visual Function

Ana Catalina Rodriguez-Martinez<sup>1-3</sup>, Vijay K. Tailor-Hamblin<sup>1,2,4</sup>,  
Michael D. Crossland<sup>1</sup>, Bethany E. Higgins<sup>1</sup>, Enzo Blindow, Tessa M. Dekker<sup>1,4</sup>,  
John A. Greenwood<sup>4</sup>, Robert H. Henderson<sup>1-3</sup>, Pete R. Jones<sup>1,2,5,\*</sup>, and  
Mariya Moosajee<sup>1,2,6,\*</sup>

<sup>1</sup> UCL Institute of Ophthalmology, London, UK

<sup>2</sup> Moorfields Eye Hospital NHS Foundation Trust, London, UK

<sup>3</sup> Great Ormond Street Hospital for Children NHS Foundation Trust, London, UK

<sup>4</sup> Experimental Psychology, University College London, London, UK

<sup>5</sup> Department of Optometry & Visual Sciences, School of Health & Psychological Sciences, City, University of London, London, UK

<sup>6</sup> The Francis Crick Institute, London, UK

**Correspondence:** Mariya Moosajee, UCL Institute of Ophthalmology, 11-43 Bath Street, London EC1V 9EL, UK. e-mail: [m.moosajee@ucl.ac.uk](mailto:m.moosajee@ucl.ac.uk)

**Received:** August 13, 2024

**Accepted:** October 27, 2024

**Published:** December 19, 2024

**Keywords:** *CRB1*; retinal dystrophy; contrast sensitivity; outcome metrics; *CRB1*-retinopathies

**Citation:** Rodriguez-Martinez AC, Tailor-Hamblin VK, Crossland MD, Higgins BE, Blindow E, Dekker TM, Greenwood JA, Henderson RH, Jones PR, Moosajee M. Assessing contrast sensitivity function in *CRB1*-retinopathies: Exploring child-friendly measures of visual function. *Transl Vis Sci Technol.* 2024;13(12):33. <https://doi.org/10.1167/tvst.13.12.33>

**Purpose:** Mutations affecting the *CRB1* gene can result in a range of retinal phenotypes, including early onset severe retinal dystrophy/Leber congenital amaurosis (EOSRD/LCA), retinitis pigmentosa, cone-rod dystrophy (CORD), and macular dystrophy (MD). As research into treatment strategies advances towards clinical translation, there is a need to establish reliable outcome metrics. This study explores the contrast sensitivity function (CSF) across different spatial frequencies in individuals with *CRB1*-retinopathies using the child-friendly PopCSF test, an iPad-based "gamified" assessment.

**Methods:** Prospective cross-sectional study of 20 patients with molecularly confirmed biallelic *CRB1* pathogenic variants from Moorfields Eye Hospital, London, UK, was conducted. Best-corrected visual acuity (BCVA), contrast sensitivity using the Pelli-Robson chart, and the PopCSF test were performed.

**Results:** Of the 20 *CRB1* patients, seven had EOSRD/LCA, three had CORD, and 10 had MD. There was no statistically significant difference between the mean BCVA between phenotypes ( $P = 0.066$ ). However, a significant difference was found between groups in the mean letter log contrast sensitivity (logCS) and area under the contrast sensitivity function (AUCSF) with  $P = 0.047$  and  $P < 0.001$ , respectively. A moderate positive correlation was observed between Pelli-Robson and PopCSF ( $r = 0.53$ ,  $P = 0.020$ ). The *CRB1* cohort had significantly lower CSF at both low and high spatial frequencies compared to controls. Among the *CRB1* phenotypes, patients with EOSRD/LCA, exhibited the lowest CSF.

**Conclusions:** This study is the first to examine CSF across spatial frequencies in patients with *CRB1*-retinopathies using the novel PopCSF test.

**Translational Relevance:** The CSF holds promise as a potential functional vision trial endpoint.

## Introduction

Biallelic pathogenic variants in the Crumbs cell polarity complex component 1 gene (*CRB1*, OMIM

no. 604210) give rise to a varied clinical spectrum of retinopathies. The most common phenotype reported is Leber congenital amaurosis (OMIM no. 613935, LCA8) accounting for 7% to 17% of cases, followed by 3% to 9% autosomal recessive retinitis pigmentosa

(OMIM no. 600105, RP12), and rarer cone-rod dystrophies (CORD) and macular dystrophies (MD),<sup>1-3</sup> for which exact prevalence statistics are sparse. *CRB1* retinopathies are characterized by distinctive features such as nummular pigmentation, fine yellow punctate deposits, preserved para-arteriolar retinal pigment epithelium, coarse and thickened retina<sup>4</sup> with some cases presenting with a Coats-like vasculopathy,<sup>5</sup> and foveal hypoplasia.<sup>6</sup> More than 300 causative variants have been identified to cause *CRB1*-related retinopathies, with the only known genotype-phenotype correlation to date being the in-frame deletion *c.498\_506del p.Ile167\_Gly169del* associated with MD.<sup>3,7,8</sup>

The *CRB1* gene codes for a transmembrane protein presenting three human isoforms: CRB1-A, CRB1-B, and CRB1-C.<sup>9</sup> The CRB1-A plays a pivotal role in retinal development and is primarily expressed in Müller glia cells. The CRB1-B isoform exhibits predominant expression in photoreceptors contributing significantly to long-term retinal integrity in adult retina, whereas the CRB1-C function remains uncertain.<sup>9</sup> CRB1 acts as a vital regulator of cellular processes, including apical-basal polarity, outer limiting membrane integrity, cell-cell adhesion, apical membrane size regulation, and cellular signaling pathways, crucial for retinal development and long-term integrity,<sup>10</sup> particularly in maintaining zonula adherence junctions at the external limiting membrane (ELM), which contributes to vascular integrity.<sup>10,11</sup> Promising advancements in potential treatments for *CRB1*-retinopathies are underway. A preclinical study using patient-derived retinal organoids from *CRB1*-retinitis pigmentosa individuals have revealed restoration of the histological retinal phenotype by showing an elevated number of photoreceptor nuclei and reduced number of nuclei protruding above the outer limiting membrane after adeno-associated viral (AAV)-mediated gene augmentation.<sup>12</sup> Another preclinical investigation found that administering AAV-CRB2 to both Müller glial cells and photoreceptors improved retinal function and structure in *Crb1* mouse models with a mid-stage disease phenotype of RP.<sup>13</sup> As research on treatment strategies advances, there is an urgency to establish reliable clinical trial outcome metrics, particularly in the pediatric population where therapies may have a larger impact.

Although distance visual acuity using logMAR or ETDRS letters has been the predominant outcome metric in both the routine clinical setting and in clinical trials, it is not a comprehensive characterization of visual function, and may fail to reveal subtle changes in visual function and its inherent variability.<sup>14,15</sup> Alternative measures of visual function have

therefore been investigated, including dark adaptation, microperimetry, contrast sensitivity, multifocal ERG, photo-stress recovery time, cone-mediated flicker sensitivity, photopic or scotopic light sensitivity and the multi-luminance mobility test.<sup>16</sup> Structural endpoints from spectral domain optical coherence tomography, fundus autofluorescence and adaptive optics scanning laser ophthalmoscopy have also been investigated.<sup>14,17,18</sup> However, regulatory bodies are still in the process of establishing a functional endpoint that holds significance for patients' visual function.<sup>16,19</sup>

Contrast sensitivity is defined as the inverse of the minimum difference in luminance required to distinguish an object from its background.<sup>20</sup> It constitutes a fundamental aspect of visual performance and is linked to the ability to perform tasks such as driving, reading and navigation.<sup>21</sup> The Pelli-Robson contrast sensitivity letter chart, first introduced in 1988, stands as the most widely used test to measure contrast sensitivity.<sup>14</sup> In this test, all letters are standardized to the size of 4.8 cm and when tested at 1 m correspond to a Snellen equivalent of approximately 20/650 (4/125).<sup>14</sup> However, the Pelli-Robson chart is only designed to provide a quick summary measure of overall contrast sensitivity (i.e., does not quantify sensitivity separately at each spatial frequency), requires the ability to read letters, and may not sustain interest in young children.<sup>22</sup>

In comparison, the contrast sensitivity function (CSF) describes spatial vision over the whole range of spatial frequencies, and can be a sensitive test for many physiological and pathological processes.<sup>23</sup> The CSF can be summarized by the area under the curve (AUC), with a higher AUC value indicating a greater overall vision.<sup>22</sup> Normative data values indicate an AUC of 1.58.<sup>24</sup> In order to improve long test durations and test compliance in the pediatric population, more efficient psychophysical tests have been developed using Bayesian adaptive algorithms (e.g. qCSF, QUEST+26).<sup>14,22,25,26</sup> These allow for identification and measurements of reduced visual sensitivity at specific spatial frequencies, as well as global changes specific to the type of retinal disease.<sup>14</sup> This holds significant relevance since regulatory bodies indicate a willingness to consider changes in contrast sensitivity for drug approvals, provided they occur across multiple frequencies.<sup>16</sup> The PopCSF is one such test: an iPad-based “gamified” assay designed to assess contrast sensitivity by “popping” (pressing) Gabor patches of varying contrast sensitivity and spatial frequency (Fig. 1A). PopCSF was previously evaluated for feasibility in children aged 4 to 9 years with amblyopia.<sup>22,27</sup> A subsequent study involving children aged five to 15 years with amblyopia, visual impairment,

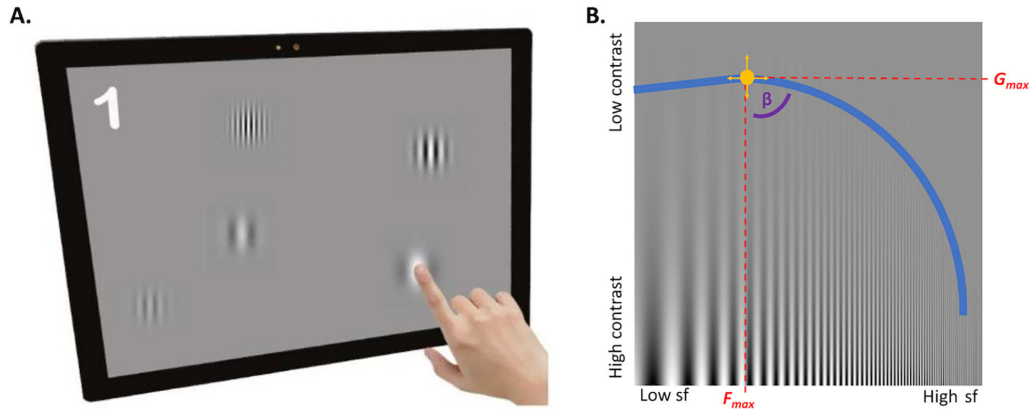


**Figure 1.** (A) An iPad-based PopCSF test. Participants “popped” Gabor patches of varying contrast and spatial frequency as they moved around the screen (courtesy of Elfadaly Det al.<sup>22</sup>). (B) A depiction of the contrast sensitivity function, shown with a sine-wave grating stimulus where its spatial frequency increases along the x-axis and contrast/amplitude decreases on the y-axis. The constructed AUCSF is depicted by the blue line, with contrast sensitivity plotted on the y-axis and spatial frequency (*sf*) on the x-axis (which should correspond with the point at which the depicted sine wave becomes difficult to detect against the background). The yellow circle shows the  $G_{max}$ , which is the peak contrast sensitivity and its spatial frequency ( $F_{max}$ ). The  $\beta$  indicates the angle of decline of the CSF after  $G_{max}$  (courtesy of Crossland et al.<sup>27</sup>).

and a control group demonstrated its practicality in a non-clinical setting, with promising results.<sup>27</sup> The aim of this study is to examine the CSF and determine whether individuals with *CRB1*-related retinopathies exhibit generalized or specific spatial frequency reductions using the novel child-friendly PopCSF test.

## Methods

This was a prospective study at a single tertiary referral center (Moorfields Eye Hospital NHS Foundation Trust, London, UK). Potential subjects were identified from the Moorfields Eye Hospital Inherited Eye Disease Database and invited to participate in a natural history study of *CRB1* retinopathies. Patients and relatives gave written informed consent for genetic testing, through the Genetic Study of Inherited Eye Disease. The study received ethical approval from the Moorfields Eye Hospital NHS Foundations Trust and the National Research Ethics Committee (Research Ethics Number: 12/LO/0141). All procedures were conducted in adherence to the tenets of the Declaration of Helsinki. The methodology of genetic testing and variant interpretation at Moorfields has been described previously.<sup>6</sup> The inclusion criteria were molecularly confirmed biallelic (pathogenic or likely pathogenic) variants in the *CRB1* gene and a visual acuity in the better seeing eye of equal or better than 1.00 logMAR. The chosen cutoff vision score was intended to ensure that the included patients can perform tests

requiring fixation stability, including psychophysical assessments.

## Clinical

Demographics, clinical data, past medical and ophthalmic history, refractive error, funduscopy, and ETDRS chart best-corrected visual acuity (BCVA) were collected from full ophthalmic assessments conducted at each visit. Patients were categorized into different phenotypes based on clinical data, retinal imaging, electrophysiology and age of onset, and grouped as early onset severe retinal dystrophy/Leber congenital amaurosis (EOSRD/LCA), macular dystrophy (MD), cone-rod dystrophy (CORD), or retinitis pigmentosa (RP).

## Clinical Tests

Best-corrected visual acuity (BCVA) measurements were captured with the Early Treatment of Diabetic Retinopathy Study (ETDRS) ESV-3000 chart by Precision Vision (Ferris et al. 1982; Ferris & Bailey 1996). Optotype contrast sensitivity was measured using a Pelli–Robson chart (Precision Vision, Woodstock, IL, USA) tested at 1 m, performed binocularly and monocularly.

## PopCSF

The PopCSF test (Irida Health, London, UK) was conducted on an Apple iPad Pro (11-inch, 2nd gener-

ation; Apple, Cupertino, CA, USA ) with iOS 15.3. The room's overhead lights were off, and the screen brightness was set to the maximum level (background luminance: 274 cd/m<sup>2</sup>; measured using Minolta CS-100; Konica Minolta, Tokyo, Japan). The test uses a gamified approach, incorporating QUEST+26 (maximum likelihood psychophysical algorithm) combined with a largely unconstrained user interface to estimate contrast sensitivity function (CSF).<sup>22</sup> The test was done binocularly, and participants observed the screen from a distance of 50 cm, with the device adjusting stimulus size at onset based on the monitored viewing distance data from the Apple TrueDepth camera (i.e., to ensure an accurate spatial frequency on the retina, invariant of head movements). During the assessment, participants interacted by "popping" moving Gabor patches distributed randomly across the screen (Fig. 1A). Subsequently, the test constructs a CSF based on  $G_{\max}$  (peak contrast sensitivity),  $F_{\max}$  (peak spatial frequency), and  $\beta$  (slope of the high-spatial-frequency drop in CSF) using an adaptive maximum likelihood algorithm (Fig. 1B). The test time was recorded as the interval between the onset of the first and the last test stimulus, identified from the device's log file.<sup>22,27</sup>

### Statistical Analysis

BCVA was converted to logarithmic minimum angle of resolution (logMAR) for statistical analysis. For the Pelli-Robson chart, log Contrast Sensitivity (logCS) values were used. For PopCSF,  $F_{\max}$ ,  $G_{\max}$  and  $\beta$  values were extracted (as above) from the log files and the Area Under the Curve (AUC) of the obtained contrast sensitivity function was calculated using a bespoke MATLAB program (MathWorks, Inc., Natick, MA, USA) (Fig. 1B). Normative data from a pediatric population ( $n = 20$ ) aged six to 14 years and adults ( $n = 202$ ) aged 18–30 years to obtain the AUC were extracted from the PopCSF iPad device and analyzed. Furthermore, a median weighted analysis was performed using normative data from participants aged 18–39 years, as reported by Dekker et al.<sup>28</sup> The resulting values were plotted to generate an AUC, allowing comparison with the contrast sensitivity functions to the *CRBI* cohort. Binocular Pelli-Robson and PopCSF comparison was chosen for all analyses. Test accuracy was determined by Pearson's correlation with the reference standard (Pelli-Robson letter contrast sensitivity). However, it is important to note that these tests are not entirely comparable, as PopCSF measures contrast sensitivity at different spatial frequencies, whereas Pelli-Robson assesses it for letters with spatial frequencies clustered around 2 to

5 cycles per degree (the expected peak of the CSF). Therefore, to further assess concordance, a Pearson correlation coefficient and linear regression were calculated between Pelli-Robson and the  $G_{\max}$  value (peak contrast sensitivity) of PopCSF. Parametric variables were assessed using linear regressions and *t*-tests, while ANOVA was employed for multiple comparisons. For nonnormally distributed data, nonparametric tests were used to compare medians. Additional analysis involved grouping based on age of onset, with a distinction between 10 years or less versus more than 10 years. Statistical significance was considered if  $P < 0.05$ . All statistical analyses were completed using GraphPad Prism (version 8.0.0; GraphPad Software, San Diego, CA, USA) and R (version 3.3.0; R Foundation for Statistical Computing, 2016).

## Results

Nineteen patients with *CRBI*-related retinopathy from 18 unrelated families were included. Participants were aged eight to 52 years. Mean {SD} age was 26.8 {14.07} years. Eight individuals (44%) were pediatric patients (<18 years old). Thirteen (72%) were male, and six (28%) were female. In terms of ethnicity, 17 patients (90%) self-identified as white, and one as black (5%). Based on clinical data, retinal imaging, and age of onset, seven patients were classified as EOSRD/LCA, two as CORD, and 10 as MD. Full details of demographic characteristics of this cohort are reported in the Table.

### Visual Acuity

Mean {SD} BCVA was 0.57 {±0.38} logMAR for the right eye, and 0.46 {±0.38} logMAR for the left. Because the visual function of both eyes was not significantly different in all individuals ( $P = 0.391$ ), the right eye was chosen for the BCVA analysis. Regarding phenotypes, the mean {SD} BCVA was 0.57 {±0.34} logMAR (confidence interval [CI], 0.25–0.89) in the LCA/EOSRD group, 0.42 {±0.34} logMAR (CI, 0.16–0.68) in the MD group, and 1.14 {±0.368} logMAR (CI, –2.16–4.44) in the CORD group. There was no statistically significant difference of the mean logMAR between phenotype groups ( $P = 0.074$ ,  $F = 3.10$ , as shown in Figure 2A).

### PopCSF and Pelli-Robson

Binocular data was chosen for the Pelli-Robson and PopCSF analysis. The mean {SD} letter logCS



**Table.** Summary of Subject Demographics, Genetic Results, and Clinical Characteristics of the 20 Patients With Biallelic Pathogenic Variants in *CRB1*

Family Number	Subject	Gender	Ethnicity	Age	Phenotype	Zygoty	Variant 1 Protein Variant 1 cDNA	Variant 2 Protein Variant 2 cDNA
45590	01	F	Black	29	MD	Homozygous	c.2506C>A	p.Pro836Thr
46120	02	F	White	17	EOSRD/LCA	Heterozygous	c.455G>A	c.3014A>T
35083	03	M	White	39	MD	Heterozygous	p.Cys152Tyr c.498_506del	p.Asp1005Val c.4142C>G
43560	04	F	White	48	MD	Heterozygous	p.Ile167_Gly169del c.498_506del	p.Pro1381Arg c.1696G>T
38236	05	M	White	47	MD	Heterozygous	p.Ile167_Gly169del c.498_506del	p.Glu556Ter c.584G>T
38229	06	M	White	24	EOSRD/LCA	Heterozygous	p.Ile167_Gly169del c.2129A>T	p.Cys195Phe c.3988del
	07	M	White	15	MD	Heterozygous	p.Glu710Val c.498_506del	p.Glu1330Serfs*11 c.1576C>T
42270	08	M	White	52	MD	Heterozygous	p.Ile167_Gly169del c.498_506del	p.Arg525* c.2401A>T
31953	09	F	White	16	EOSRD/LCA	Heterozygous	p.Ile167_Gly169del c.2548G>A	p.Lys801* c.4006-10A>G
37161	10	M	White	17	MD	Heterozygous	p.Gly850Ser c.498_506del	N/A c.2308G>T
46830	11	M	White	10	EOSRD/LCA	Heterozygous	p.Ile167_Gly169del c.2843G>A	p.Gly770Cys c.1712A>C
44092	12	F	White	11	MD	Heterozygous	p.Cys948Tyr c.498_506del	p.Glu571Ala c.2843G>A
35283	13	M	White	11	EOSRD/LCA	Homozygous	p.Ile167_Gly169del c.2843G>A	p.Cys948Tyr
35283	14	M	White	8	EOSRD/LCA	Homozygous	c.2843G>A	p.Cys948Tyr
32038	15	M	White	40	CORD	Heterozygous	c.498_506del	c.1431delG
33707	16	M	White	29	MD	Heterozygous	p.Ile167_Gly169del c.498_506del	p.Ser478Profs*24 c.3827_3828del
47941	17	M	White	18	EOSRD/LCA	Heterozygous	p.Ile167_Gly169del c.2291G>A	p.Glu1276Valfs*4 p.Arg764His
21819	18	M	White	33	CORD	Homozygous	c.470G>C	c.2506C>A
35229	19	F	White	34	MD	Heterozygous	p.C157Sp.Cys157Ser c.498_506del	p.Pro836Thr c.2290C>T
							p.Ile167_Gly169del	p.Arg764Cys

(Pelli-Robson) for the *CRB1* cohort were 1.41 {±0.38} (CI, 0.64–1.01), 1.23 {±0.41} for the right eye, and 1.26 {±0.51} for the left eye. The mean letter logCS (Pelli-Robson) by phenotype was 1.30 {±0.25} (CI, 1.07–1.53) for LCA/EOSRD, 1.58 {±0.26} (CI, 1.37–1.80) for MD and 0.90 {±0.85} (CI, –6.72–8.52) for CORD. There was a statistically significant difference of the mean letter logCS between phenotype groups ( $P = 0.047$ ,  $F = 3.782$ ), as shown in Figure 2B.

The test was completed successfully by the 19 participants. The mean AUCSF (PopCSF) for the *CRB1* cohort ( $n = 19$ ) was 0.85 {±0.45} logCS (CI, 0.63–1.007). The mean AUCSF by phenotype was 0.41 {±0.25} logCS (CI, 0.17–0.64) for LCA/EOSRD, 1.19

{±0.26} logCS (CI, 1.006–1.38) for MD and 0.71 {±0.47} logCS (CI, –3.5–4.95) for CORD. There was a statistically significant difference of AUCSF between phenotype groups ( $P < 0.001$ ,  $F = 16.54$ ), as shown in Figure 2B. As shown in Figure 3 the *CRB1* cohort had lower logCS at both low and high spatial frequencies compared to normative data, depicting an overall significantly lower CSF. Patients with MD exhibited higher logCS at lower spatial frequencies compared to the other phenotypes, with the slope declining relatively consistently across different spatial frequencies thereafter. Patients with EOSRD/LCA demonstrated the poorest CSF by demonstrating the lowest logCS at lower spatial frequencies with a subsequent sharp decline at low

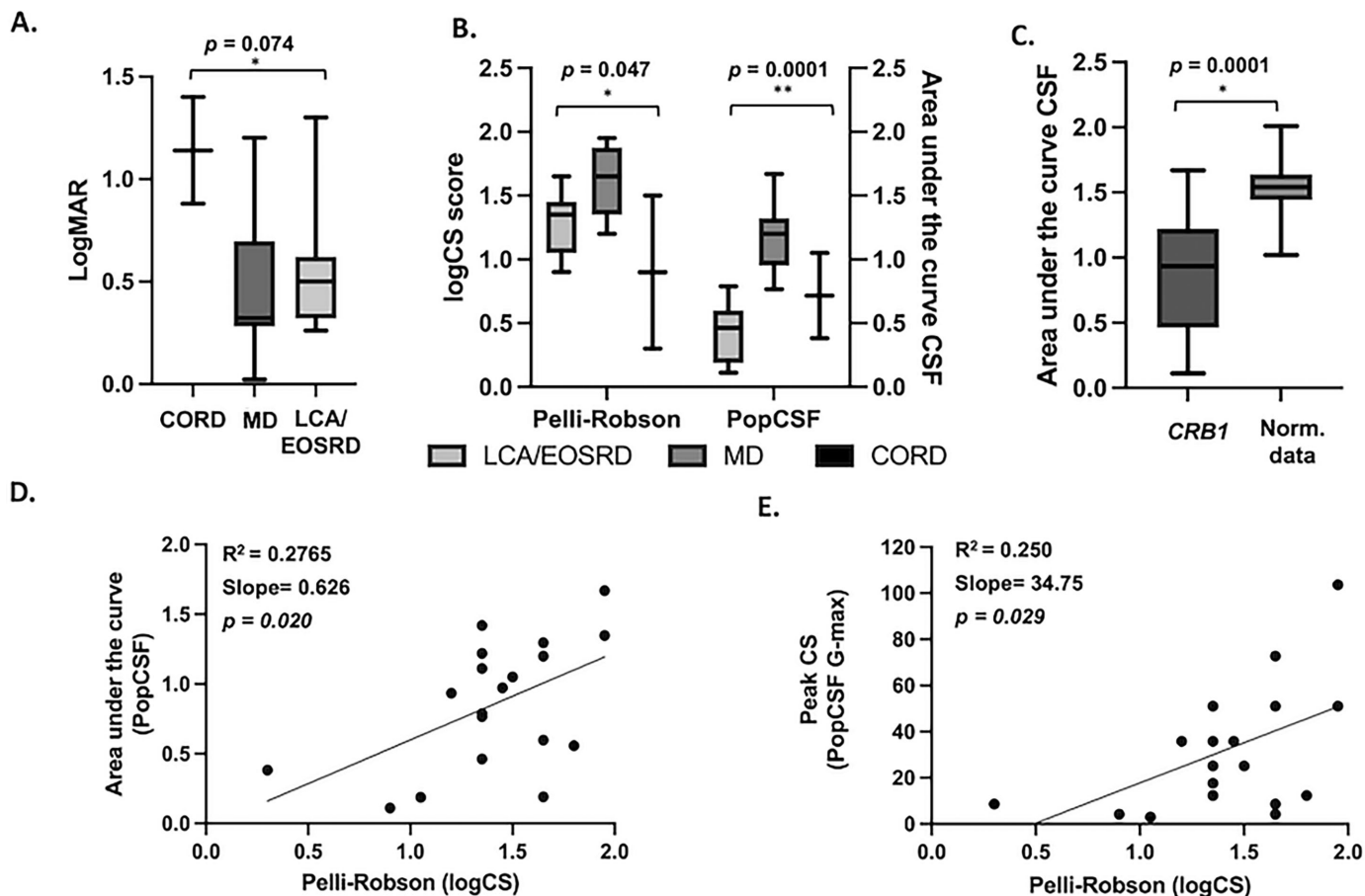


**Figure 2.** (A) Box plot showing BCVA levels in logMAR units, separately according to phenotypes in the *CRB1* cohort. CORD (1.40 logMAR, SD  $\pm 0.36$ ), MD (0.42 logMAR, SD  $\pm 0.34$ ), and LCA/EOSRD (0.57 logMAR, SD  $\pm 0.34$ ). There was no statistically significant difference in the mean logMAR between phenotype groups ( $*P = 0.074$ ,  $F$  value 3.10) (B) Box plot illustrating contrast sensitivity across both tests and subgroups. Y-axes depiction of logCS for the Pelli-Robson chart and AUCSF for PopCSF, separately for *CRB1* phenotypes. Values show a significant difference between groups ( $*P = 0.0474$ ,  $F$  value 3.78;  $**P = 0.0001$ ,  $F$  value 16.54) respectively. (C) Mean AUCSF from the PopCSF in *CRB1* patients was 0.85 (SD  $\pm 0.45$ ) and 1.51 (SD  $\pm 0.19$ ) in normative data, showing a statistically significant difference ( $*P = 0.0001$ ). (D) Scatterplot from *CRB1* patients showing the relationship between logCS (Pelli-Robson) and AUCSF (PopCSF). Linear regression was made showing a positive correlation between both tests ( $R^2 = 0.276$ ; slope 0.6265;  $P = 0.0207$ ; CI, 0.78–1.81). (E) Scatterplot from *CRB1* patients showing the relationship between logCS (Pelli-Robson) and peak of CS (PopCSF G-max). Linear regression was made showing a positive correlation between both tests ( $R^2 = 0.250$ ; slope 34.75;  $P = 0.029$ ; CI, 4.01–65.49).

spatial frequencies. Those in the CORD group showed more intermediate losses. The  $\beta$  values, which represent the steepness of the CSF decline after the peak contrast sensitivity ( $G_{max}$ ), were calculated for each group. The results showed mean  $\beta$  (angle of decline) values of 1.00  $\{\pm 0.0\}$  for CORD, 2.  $\{\pm 0.92\}$  for EOSRD/LCA, and 2.73  $\{\pm 0.64\}$  for MD. These findings confirm that the MD group had the most gradual decline in contrast sensitivity across spatial frequencies.

Normative data showed a mean AUCSF of 1.52  $\{\pm 0.16\}$  logCS (CI, 1.50–1.54) (Fig. 2C). There was a statistically significant difference when comparing the mean AUCSF of the *CRB1* group to normative data ( $P < 0.001$ ,  $t_{219} = 11.93$ ). There was a

moderate positive correlation between Pelli-Robson and the AUCSF of the PopCSF  $r = 0.5259$ ,  $P = 0.020$  (CI, 0.09–0.79). Similarly, a statistically significant moderate positive correlation between Pelli-Robson and the  $G_{max}$  value (peak contrast sensitivity) from the PopCSF test,  $r = 0.508$ ,  $P = 0.029$  (CI, 0.06–0.77). The median (IQR) test duration for PopCSF in the *CRB1* cohort was 126 seconds (14) and 126 (26) on the normative data. There was no statistically significant difference in test duration between the two groups ( $P = 0.895$ ). Additionally, there was no statistically significant difference in test time when comparing pediatric population 127 (23.5) versus adults 122 (16.5) of the *CRB1* cohort ( $P = 0.285$ ).

Contrast sensitivity functions

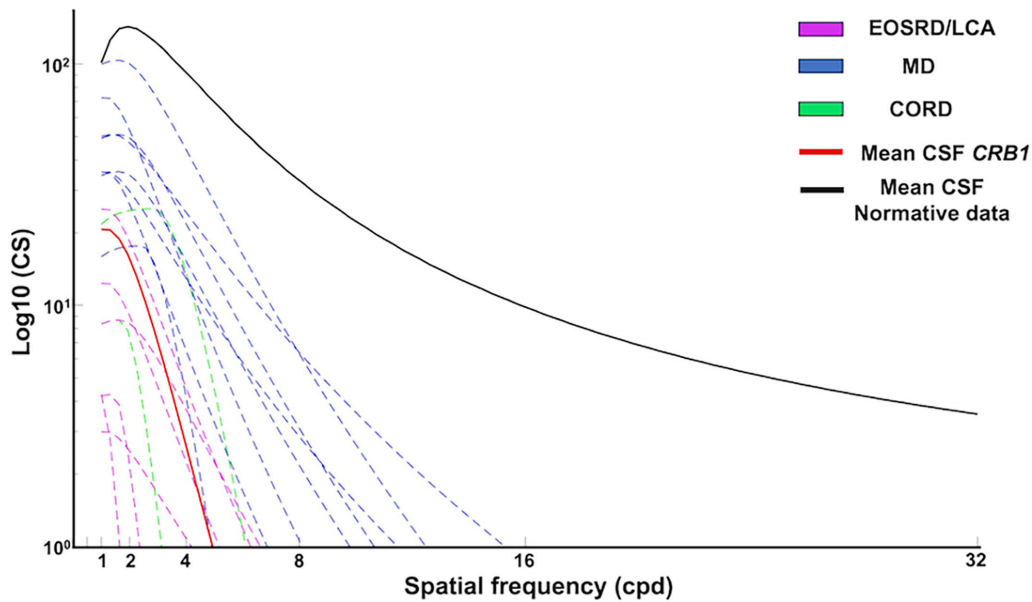


**Figure 3.** Plots of the CSF in the *CRB1* cohort, with contrast sensitivity plotted on the y-axis (in log10 units) and spatial frequencies (in cycles per degree) on the x-axis. The red line represents the mean CSF of the *CRB1* cohort, and the black line represents the mean CSF from normative data collated from Dekker et al. The *CRB1* cohort had lower logCS at both low and high spatial frequencies compared to normative data, depicting an overall significantly lower CSF. Among the *CRB1* phenotypes, patients with MD, indicated in blue, exhibited higher logCS at lower spatial frequencies compared to the other phenotypes, with the slope declining relatively consistently across different spatial frequencies thereafter. By contrast, patients with EOSRD/LCA, depicted in magenta, demonstrated the lowest CSF, by exhibiting the lowest logCS at lower spatial frequencies and a subsequent sharp decline at low spatial frequencies, indicating substantial losses in sensitivity to high frequencies. Similarly, the CORD group, represented in green, showed a sharp decline with increasing spatial frequency.

Age of Onset and CSF

Participants were also grouped based on age of onset ( $\leq 10$  years vs.  $> 10$  years). For those with a disease onset  $\leq 10$  years ( $n = 11$ , 7 LCA/EOSRD,

2 MD, 1 CORD), the mean AUCSF was  $0.61 \{\pm 0.41\}$  (CI, 0.33–0.89), whereas for those with an onset  $> 10$  years ( $n = 8$ , 7 MD, 1 CORD), the mean AUC was  $1.18 \{\pm 0.28\}$  (CI, 0.94–1.42) indicating a worse CSF in those with early onset compared to those with later

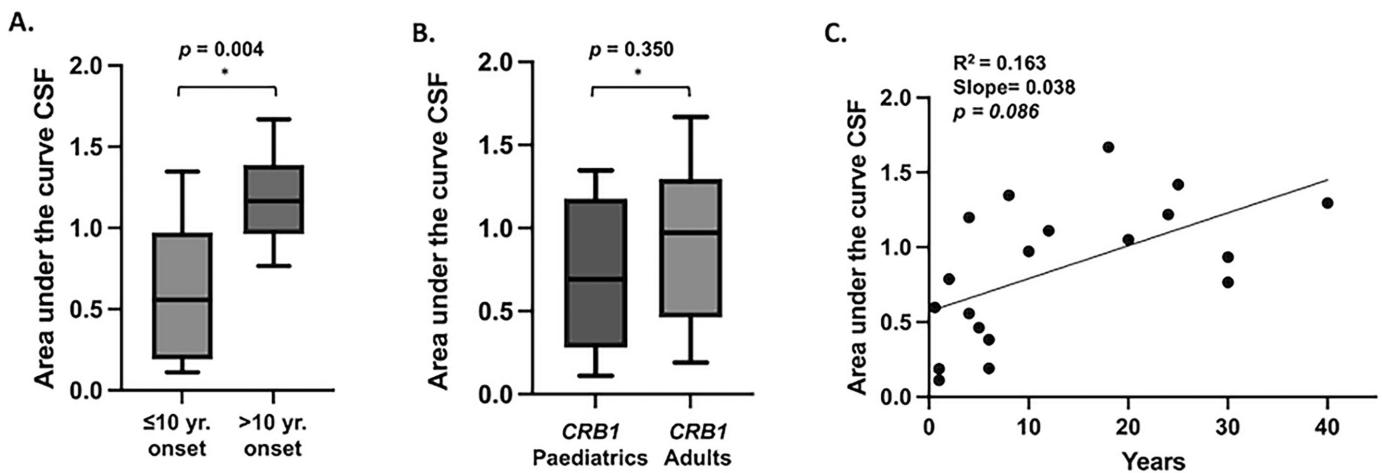


**Figure 4.** (A) A statistically significant difference in the mean AUCSF was observed ( $P = 0.004$ ,  $t_{17} = 3.31$ ,  $df = 17$ ) when grouping based on age of onset, with a distinction between onset  $\leq 10$  years versus  $> 10$  years, with the former having a worse CSF compared to those with later disease onset. (B) No statistically significant difference in mean AUCSF was observed when comparing pediatric individuals versus adults ( $P = 0.350$ ). (C) Linear regression revealed a slight positive correlation between AUCSF and age, indicating higher AUCSF is associated with older age ( $R^2 = 0.163$ ; slope 0.038;  $P = 0.086$ ; CI, 0.02–0.05).

disease onset (Fig. 4A). This difference in the mean AUCSF was statistically significant ( $P = 0.004$ ,  $t_{17} = 3.31$ ). There was no statistically significant difference in AUCSF when comparing pediatric population versus adults of the *CRB1* cohort ( $P = 0.350$ ,  $t_{17} = 0.96$ ), as shown in Figure 4B. Ultimately, linear regression showed a slight positive correlation between AUCSF and age, indicating that older age is associated with a higher AUCSF ( $R^2 = 0.163$ , slope 0.038,  $P = 0.086$  (CI, 0.02–0.05) (Fig. 4C).

## Discussion

The present study reports CSF data in patients with molecularly confirmed *CRB1*-related retinopathy. The results were subsequently compared to normative data and to the current clinical reference standard for contrast sensitivity (Pelli-Robson). Although the two tests are not entirely comparable, there was a moderate positive correlation between them, which opens the possibility of using more child-friendly tests to measure the contrast sensitivity function in individuals with inherited retinal diseases (IRDs).

The *CRB1* gene is involved in the development and maintenance of the retina.<sup>6</sup> When disrupted, it results in various phenotypes, including EOSRD/LCA, RP, CORD, and MD.<sup>3</sup> Reported BCVA levels across different cohorts range from 1.13 logMAR for individuals with the LCA/EOSRD phenotype,<sup>6</sup> 0.8 and 0.7 logMAR in cohorts predominantly including RP patients, to 0.3 logMAR in cohorts including MD patients.<sup>1,2,8</sup> Recent advances in potential treatments for *CRB1*-related retinopathies have shown promising results in preclinical studies. AAV) vector-mediated h*CRB1* gene augmentation in Müller glial and photoreceptor cells partially restored the histological phenotype and transcriptomic profile of *CRB1* in hiPSC derived retinal organoid models.<sup>12</sup> A further preclinical study revealed that administering AAV-*CRB2* to both Müller glial cells and photoreceptors enhanced retinal function and structure in *Crb1* mouse models exhibiting a mid-stage disease phenotype of RP.<sup>13</sup> As the field progresses, establishing new outcome metrics becomes crucial, prompting a shift towards more comprehensive measures that capture subtle changes in visual function and reduce inherent variability. Previous *CRB1*-retinopathy related natural history studies have shown that visual acuity and visual fields remain relatively stable over a 2-year period.<sup>1</sup> Alternatively, microperimetry has proven useful for documenting and monitoring residual retinal function

in *CRB1* patients by reporting the number of seeing loci and tracking disease progression using both foveal (6°) and macular (10-2) grids.<sup>1,29</sup> Other structural parameters such as macular volume profile including the ratio of perifoveal-to-foveal retinal volume have been proposed as valuable indicators.<sup>29</sup> However, none of the previous *CRB1* studies have explored the role of contrast sensitivity nor child-friendly tests suitable for the pediatric population as potential outcome metrics.

Visual acuity, the most common vision test, may not be ideal for characterizing functional deficits because it can be insensitive in the early stages of retinal degeneration or show a slow decline that can be impractical over shorter follow-up periods.<sup>30</sup> Instead, contrast sensitivity has been reported to correlate better with subjective visual impairment and vision related quality of life compared to visual acuity, as well as being affected earlier in the course of neurodegenerative disorders and potentially allowing the detection of more subtle changes in visual function.<sup>14</sup> Oishi et al.<sup>31</sup> reported that contrast sensitivity measurements, using Contrast Sensitivity Accurate Tester (CAT-2000; Neitz, Tokyo, Japan), in RP patients were reduced even when their visual acuity losses were mild. Similarly, Xiong et al. reported that even when visual acuity was relatively normal (<0.3 logMAR) in their study groups, including individuals with cataracts, glaucoma, age-related macular degeneration, and RP, early contrast sensitivity deficits were noted, with the RP group experiencing the most significant deficits (1.20 logCS  $\pm$ 0.50) when testing with Pelli-Robson. This study hypothesized that in the RP cases with relatively normal vision, the CS deficits may be related to a uniform increase in intercone spacing in the fovea, enlargement of cone inner segments leading to increased optical bandwidth of cones, or light leakage between foveal cones.<sup>32</sup>

Although testing contrast sensitivity using Pelli-Robson chart can detect subtle changes compared to ETDRS chart, it restricts measurements to a limited set of spatial frequencies and may consequently underestimate deficits in contrast sensitivity and overall visual function.<sup>22</sup> Instead, contrast sensitivity function enables the identification and measurement of reduced contrast sensitivity at specific spatial frequencies, as well as global changes related to the specific type of retinal disease, which provides a more comprehensive analysis of visual function.<sup>14</sup> Analyses of contrast sensitivity function measured at various spatial frequencies in patients with RP have identified reductions at both low and high spatial frequencies; yet deficits were more commonly observed at the higher



spatial frequencies.<sup>31</sup> In our cohort, the CSF was significantly lower when compared to normative data at both lower and higher spatial frequencies. Among the *CRB1* phenotypes, patients with MD exhibited higher logCS at lower spatial frequencies, with the slope declining relatively consistently across different spatial frequencies thereafter. Conversely, patients with EOSRD/LCA and CORD exhibited lower logCS at lower spatial frequencies followed by a sharp decline at higher spatial frequencies, depicting a worse visual function. When conducting subsequent analysis and comparing groups primarily with macular involvement (MD, CORD) to those with LCA/EOSRD, a significant difference in CSF was seen, with the latter exhibiting more impairment. It is important to highlight that the PopCSF measures contrast sensitivity across a larger expanse of the visual field, where targets drift around the entire screen, covering approximately 40 degrees of visual angle<sup>27</sup> which can assess extrafoveal retinal loci. This could explain why the LCA/EOSRD group, characterized by a more pronounced generalized retinal degeneration, demonstrated markedly worse CSF compared to patients primarily affected by macular conditions.<sup>3,6</sup>

Although patients with MD in this *CRB1* cohort showed a marked impairment in visual acuity of 0.57 logMAR {SD  $\pm$  0.34} and CSF (AUCSF 1.19 {SD  $\pm$  0.26}), significant reductions in CSF assessed using qCSF have been reported even with good visual acuity in the presence of macular disease.<sup>33</sup> Similarly, individuals with proven IRDs and BCVA 0.3 logMAR or better, assessed for CSF using qCSF, have exhibited deficits in contrast sensitivity despite mild visual acuity loss.<sup>24</sup> Interestingly, even though the BCVA were comparable among different IRDs groups, most pronounced deficits were observed in patients with Stargardt's disease (AUCSF 0.61), followed by Best disease (AUCSF 1.23) and rod-cone dystrophy (AUCSF 1.27) in comparison to controls (AUCSF 1.58). Comparably, the BCVA in this study was similar between all phenotype groups. However, differences emerged when CSF was assessed, with a more pronounced deficit in the EOSRD/LCA group. This demonstrates that the CSF is not simply interchangeable with visual acuity—rather, the CSF can provide more comprehensive information about visual dysfunction than visual acuity alone. Our findings further suggest that methods such as the PopCSF are a promising clinical tool for quantifying subtle visual deficits that might be overlooked by existing testing methods.

Despite the widespread use of the Pelli-Robson test, it is only designed to provide a quick summary measure of overall contrast sensitivity, and it may

not sustain interest in young children.<sup>20,22</sup> Efforts to improve efficiency and compliance in measuring CSF in the pediatric population led to the development of the PopCSF test. This novel, child-friendly approach uses adaptive algorithms to assess contrast sensitivity through an engaging optotype test and bubble-popping game. PopCSF has been tested in healthy controls, children with amblyopia and with other causes of visual impairment (RP, achromatopsia, albinism, optic nerve hypoplasia) and has demonstrated its practicality in non-clinical settings, making it a promising tool for assessing contrast sensitivity in children.<sup>27</sup> In the context of IRDs, this study is the first to employ the PopCSF test in a *CRB1*-retinopathy cohort to measure CSF across different spatial frequencies. This is highly relevant as regulatory bodies denote that contrast sensitivity can only be used as a functional endpoint in clinical trials if significant changes are reported across multiple frequencies.<sup>16</sup> In addition, the test feasibility, as indicated by completion rates, was 100%, a measure that holds particular importance when conducting assessments in the pediatric cohort. Ultimately, the test duration in the pediatric cohort did not exceed that of adults or healthy controls, suggesting that visually impaired patients of any age can easily perform the investigation.

## Strengths and Limitations

*CRB1*-retinopathies represent a rare subset of the inherited retinal disease population, and whereas this study is among the largest case series, the sample size remains small, with limitations in statistical power and sample heterogeneity. It is noteworthy that the PopCSF and Pelli-Robson tests are not entirely comparable, as PopCSF measures contrast sensitivity across different spatial frequencies, whereas the Pelli-Robson assesses CSF at a single spatial frequency. Hence, to further assess the correlation, a Pearson correlation coefficient was calculated between Pelli-Robson and the  $G_{\max}$  value of PopCSF, which showed a clear correlation between the two. Additional distinctions between Pelli-Robson and PopCSF include the latter's focus on detection rather than identification. Although PopCSF is designed to be engaging for children, it lacks precise control over stimulus location on the retina, as the targets appear and move freely across any part of the screen. Therefore visual field defects could influence how stimuli are perceived across different retinal areas, potentially impacting the PopCSF results. Test reliability (test-retest repeatability) was not assessed on this study, but this has been previously established.<sup>27</sup> Pelli-Robson was performed both

binocularly and monocularly, but direct comparison was made binocularly for PopCSF, which was performed as a binocular test. It could be recommended to perform both tests unilaterally to assess disease progression; however, most IRDs tend to be symmetrical.

## Conclusions

This study explores the CSF across different spatial frequencies among individuals with *CRB1*-related retinopathies. We observed clear losses in contrast sensitivity that were evident across both low and high spatial frequencies, and clear differences amongst the *CRB1* phenotypes, with the LCA/EOSRD being the most affected. Using a functional outcome metric with better sensitivity compared to visual acuity can improve the detection of subtle changes in visual function over time. The CSF can hold potential as a functional vision endpoint for clinical trials and routine monitoring. It is linked to everyday functional vision and displays potential for tracking the advancement of sight loss in various eye diseases or improvements with treatment/intervention.<sup>30</sup> Additional *CRB1* prospective natural history studies are necessary for global consensus and robust evidence. Critical considerations for potential trial points encompass sensitivity to disease changes, reproducibility, and correlation with other measures of disease stage.<sup>34</sup>

## Acknowledgments

The authors thank the Wellcome Trust 205174/Z/16/Z, Fight for Sight, Moorfields Eye Charity and the NIHR Biomedical Research Centre at Moorfields Eye Hospital NHS Trust and UCL Institute of Ophthalmology. The sponsor and funding organisation had no role in the design or conduct of this research.

Supported by Moorfields Eye Charity Springboard Award no. GR001216.

Disclosure: **A.C. Rodriguez-Martinez**, None; **V.K. Tailor-Hamblin**, None; **M.D. Crossland**, None; **B.E. Higgins**, None; **E. Blindow**, None; **T.M. Dekker**, None; **J.A. Greenwood**, None; **R.H. Henderson**, None; **P.R. Jones**, None; **M. Moosajee**, None

\* PRJ and MM are joint last authors.

## References

1. Nguyen XT, Talib M, van Schooneveld MJ, et al. *CRB1*-associated retinal dystrophies: a prospective natural history study in anticipation of future clinical trials. *Am J Ophthalmol*. 2022;234:37–48.
2. Talib M, Van Cauwenbergh C, De Zaeytijd J, et al. *CRB1*-associated retinal dystrophies in a Belgian cohort: genetic characteristics and long-term clinical follow-up. *Br J Ophthalmol*. 2022;106:696–704.
3. Varela MD. *CRB1*-associated retinal dystrophies: genetics, clinical characteristics, and natural history. *Am J Ophthalmol*. 2023;246:107–121.
4. Jacobson SG, Cideciyan AV, Aleman TS, et al. Crumbs homolog 1 (*CRB1*) mutations result in a thick human retina with abnormal lamination. *Hum Mol Genet*. 2003;12:1073–1078.
5. Henderson RH, Mackay DS, Li Z, et al. Phenotypic variability in patients with retinal dystrophies due to mutations in *CRB1*. *Br J Ophthalmol*. 2011;95:811–817.
6. Rodriguez-Martinez AC, Higgins BE, Tailor-Hamblin V, et al. Foveal hypoplasia in *CRB1*-related retinopathies. *Int J Mol Sci*. 2023;24(18):13932.
7. Owen N, Toms M, Tian Y, et al. Loss of the crumbs cell polarity complex disrupts epigenetic transcriptional control and cell cycle progression in the developing retina. *J Pathol*. 2023;259:441–454.
8. Khan KN, Robson A, Mahroo OAR, et al. A clinical and molecular characterisation of *CRB1*-associated maculopathy. *Eur J Hum Genet*. 2018;26:687–694.
9. Mairot K, Smirnov V, Bocquet B, et al. *Crb1*-related retinal dystrophies in a cohort of 50 patients: a reappraisal in the light of specific müller cell and photoreceptor *crb1* isoforms. *Int J Mol Sci*. 2021;22(23):12642.
10. Boon N, Wijnholds J, Pellissier LP. Research models and gene augmentation therapy for *CRB1* retinal dystrophies. *Front Neurosci*. 2020;14:860.
11. Stehle IF, Inventarza JA, Woerz F, et al. Human *CRB1* and *CRB2* form homo- and heteromeric protein complexes in the retina. *Life Sci Alliance*. 2024;7(6):e202302440.
12. Boon N, Lu X, Andriessen CA, et al. AAV-mediated gene augmentation therapy of *CRB1* patient-derived retinal organoids restores the histological and transcriptional retinal phenotype. *Stem Cell Reports*. 2023;18:1123–1137.
13. Pellissier LP, Quinn PM, Alves CH, et al. Gene therapy into photoreceptors and Müller glial cells

- restores retinal structure and function in *CRB1* retinitis pigmentosa mouse models. *Hum Mol Genet.* 2015;24:3104–3118.
14. Vingopoulos F, Wai KM, Katz R, Vavvas DG, Kim LA, Miller JB. Measuring the contrast sensitivity function in non-neovascular and neovascular age-related macular degeneration: the quantitative contrast sensitivity function test. *J Clin Med.* 2021;10:2768.
  15. Yu HJ, Kaiser PK, Zamora D, et al. Visual acuity variability: comparing discrepancies between snellen and ETDRS measurements among subjects entering prospective trials. *Ophthalmol Retina.* 2021;5:224–233.
  16. Csaky K, Ferris F, 3rd, Chew EY, et al. Report from the NEI/FDA Endpoints Workshop on Age-Related Macular Degeneration and Inherited Retinal Diseases. *Invest Ophthalmol Vis Sci.* 2017;58:3456–3463.
  17. Menghini M, Cehajic-Kapetanovic J, MacLaren RE. Monitoring progression of retinitis pigmentosa: current recommendations and recent advances. *Expert Opin Orphan Drugs.* 2020;8(2–3):67–78.
  18. Taylor LJ, Josan AS, Jolly JK, MacLaren RE. Microperimetry as an outcome measure in RPGR-associated retinitis pigmentosa clinical trials. *Transl Vis Sci Technol.* 2023;12(6):4.
  19. Schmetterer L, Scholl H, Garhöfer G, et al. Endpoints for clinical trials in ophthalmology. *Prog Retin Eye Res.* 2023;97:101160.
  20. Anderson HA, Mathew AR, Cheng H. Evaluation of the SpotChecks contrast sensitivity test in children. *Ophthalmic Physiol Opt.* 2023;43:64–72.
  21. Thayaparan K, Crossland MD, Rubin GS. Clinical assessment of two new contrast sensitivity charts. *Br J Ophthalmol.* 2007;91(6):749–752.
  22. Elfadaly D, Abdelrazik ST, Thomas PB, Dekker TM, Dahlmann-Noor A, Jones PR. Can psychophysics be fun? Exploring the feasibility of a gamified contrast sensitivity function measure in amblyopic children aged 4-9 years. *Front Med (Lausanne).* 2020;7:469.
  23. Jindra LF, Zemon V. Contrast sensitivity testing: a more complete assessment of vision. *J Cataract Refract Surg.* 1989;15:141–148.
  24. Alahmadi BO, Omari AA, Abalem MF, et al. Contrast sensitivity deficits in patients with mutation-proven inherited retinal degenerations. *BMC Ophthalmol.* 2018;18:313.
  25. Watson AB. QUEST+: A general multidimensional Bayesian adaptive psychometric method. *J Vis.* 2017;17(3):10.
  26. Dorr M, Lesmes LA, Lu ZL, Bex PJ. Rapid and reliable assessment of the contrast sensitivity function on an iPad. *Invest Ophthalmol Vis Sci.* 2013;54:7266–7273.
  27. Crossland MD, Dekker TM, Dahlmann-Noor A, Jones PR. Can children measure their own vision? A comparison of three new contrast sensitivity tests. *Ophthalmic Physiol Opt.* 2024;44:5–16.
  28. Dekker TM, Farahbakhsh M, Atkinson J, Braddick OJ, Jones PR. Development of the spatial contrast sensitivity function (CSF) during childhood: Analysis of previous findings and new psychophysical data. *J Vis.* 2020;20(13):4.
  29. Roshandel D, Thompson JA, Jeffery RC, et al. Multimodal retinal imaging and microperimetry reveal a novel phenotype and potential trial endpoints in *CRB1*-associated retinopathies. *Transl Vis Sci Technol.* 2021;10(2):38.
  30. Hou F, Lesmes LA, Kim W, et al. Evaluating the performance of the quick CSF method in detecting contrast sensitivity function changes. *J Vis.* 2016;16(6):18.
  31. Oishi M, Nakamura H, Hangai M, Oishi A, Otani A, Yoshimura N. Contrast visual acuity in patients with retinitis pigmentosa assessed by a contrast sensitivity tester. *Indian J Ophthalmol.* 2012;60:545–549.
  32. Xiong YZ, Kwon M, Bittner AK, Virgili G, Giacomelli G, Legge GE. Relationship between acuity and contrast sensitivity: differences due to eye disease. *Invest Ophthalmol Vis Sci.* 2020;61(6):40.
  33. Wai KM, Vingopoulos F, Garg I, et al. Contrast sensitivity function in patients with macular disease and good visual acuity. *Br J Ophthalmol.* 2022;106:839–844.
  34. Ayala A, Cheetham J, Durham T, Maguire M. The importance of natural history studies in inherited retinal diseases. *Cold Spring Harb Perspect Med.* 2023;13(3):a041297.